Supporting Information for "On the resolution-dependence of anvil cloud fraction and precipitation efficiency in radiative-convective equilibrium"

N. Jeevanjee[1], L. Zhou[1]

[1]Geophysical Fluid Dynamics Laboratory, Princeton NJ

Contents of this file

1. Text S1 to S5
2. Figures S1 to S5
3. Table S1

Text S1 – DAM Simulations

To test the robustness of our results to the choice of cloud-resolving model, and to explore the impact of interactive radiation (which is unavailable in our FV^3 configuration), we perform additional simulations with Das Atmospharisch Modell (DAM, Romps, 2008). Similar to our primary FV^3 simulations, we run DAM RCE simulations on a fixed 72×72 horizontal grid at a variety of resolutions, comparable to the range explored for FV^3 in the main text. All other DAM configuration details are identical to those for the simulations performed in Jeevanjee and Romps (2018) and documented therein. In particular, DAM employs the six class, single-moment Lin-Lord-Krueger microphysics scheme (Lin et al.,

1983; Lord et al., 1984; Krueger et al., 1995) as well as the Rapid Radiative Transfer Module for interactive radiation (Mlawer et al., 1997).

Figure S1a shows steady-state cloud fraction profiles for these DAM RCE simulations at variable dx. As for the FV^3 simulations shown in the main text, these DAM simulations show a steady increase of anvil cloud fraction with increasing resolution. The range is not as large for DAM as it is for FV^3 (roughly 0.06-0.2, vs 0.05-0.5 for FV^3), but this is not surprising given inter-model differences in anvil cloud fraction (Wing et al., 2020). Furthermore, both DAM and FV^3 exhibit a vertical dipole-like dx-dependence of cloud fraction, with high cloud fraction increasing with resolution while low cloud fraction decreases. These qualitative similarities between DAM and FV^3, along with the fundamental nature of the physical mechanism discussed in the text, suggests that the resolution-dependence of high cloud fraction seen in this study may indeed be robust across cloud-resolving models.

A limitation of our FV^3 simulations is the absence of interactive radiation. While this helps to isolate the resolution-dependence of cloud fraction from possible radiative feedbacks, it is of interest to know whether such feedbacks might significantly affect or ameliorate this resolution-dependence. For instance, one may wonder if DAM's more muted resolution dependence of cloud fraction may be due to its interactive radiation. Figure S1c suggests that this is not the case, however, as DAM's radiative cooling profiles $Q(z)$ (units of W/m^3) do not differ markedly as dx decreases, and the column-integrated cooling $\int Q\,dz$ (units of W/m^2) only varies by 20% or so across the simulations.

To probe the impact of cloud radiative effects (CRE), we run additional DAM simulations with no CRE by applying only the clear-sky radiative heating tendencies to the

model prognostic variables. The resulting cloud fraction and radiative heating profiles are shown in Figure S1b,d. While these profiles in a given simulation do show a slight sensitivity to CRE (Harrop & Hartmann, 2016), the overall resolution sensitivity of both cloud fraction and radiative heating do not seem materially affected by CRE.

Text S2 – Vertical Velocity Thresholds

As discussed in section 2.2 of the main text, the vertical velocity threshold w_0 used to identify 'active' (i.e. updraft) cloudy regions varies with resolution, consistent with the findings of Jeevanjee (2017) and references therein. The values of $w_0(dx)$, shown in Table S1, were chosen subjectively by a combination of inspection and consistency with the results of Jeevanjee (2017) which show convergence of updraft vertical velocities in this model for $dx < 250$ m.

Text S3 – Analysis of Fixed Domain Simulations

Figure 1 of the main text primarily shows simulations on a fixed 96×96 grid, which allows for simulation over a wide range of resolutions. A drawback of this approach is that the domain size then varies with resolution. To address this we also conducted a necessarily more limited set of simulations over a fixed 96×16 km^2 domain. Cloud fraction profiles from these simulations were shown in Fig. 1, but these simulations were not analyzed further in the main text. To build confidence that the mechanism we describe is operating similarly in both the fixed domain and fixed grid simulations, Figure S2 shows the same profiles of evaporation, mass flux, etc. as in Fig. 2 of the main text, but for the fixed domain simulations. There are fewer simulations in this set, but otherwise the behavior is very similar to Fig. 2 of the main text, providing further evidence that the mechanisms are the same. Figure S3 similarly reproduces Fig. B.1 of the main text but

with our fixed domain simulations, again showing a strong similarity to the fixed grid results shown in the main text.

Text S4 – Profiles of Eddy Wind Speeds

Figure 5 of the main text shows that the mixing timescales $\kappa(dx) \sim dx/u_{\mathrm{rms}}$, where $u_{\mathrm{rms}} = 0.1$ m/s. To confirm that this is a resonable value for u_{rms}, we take daily snapshots for the last 14 days of our FV^3 fixed grid, warm-rain simulations and calculate the standard deviation of the horizontal wind u for each vertical level. The resulting u_{rms} profiles (the mean u is approximately zero) for each simulation is shown in Figure S4. While there is some dx-dependence of u_{rms}, and all values are greater than 0.1 m/s, we do see that the majority of values are indeed $O(0.1$ m/s).

Text S5 – Aggregated Simulations

One question left unanswered by the fixed-grid simulations analyzed in the main text is whether convective organization might affect the results. To probe this (without introducing additional parameters required by an external forcing, e.g. an SST gradient), we consider self-organized or 'self-aggregated' convection, a form of spontaneous organization known to appear in cloud-resolving simulations of RCE over uniform SSTs (Wing, Emanuel, et al., 2017; C. Muller, 2022).

To this end we conduct FV^3 simulations identical to the warm-rain fixed-grid simulations, but on a 'bowling-alley' 1024×96 km^2 domain to promote aggregation, following Cronin and Wing (2017); Wing, Reed, et al. (2017). Since our FV^3 simulations are not equipped with interactive radiation, found in many studies to be an important feedbacks for self-aggregation (e.g. Bretherton et al., 2005; Wing & Emanuel, 2014; C. J. Muller & Romps, 2018), we instead further promote self-aggregation by disabling rain evapora-

tion, which inhibits cold pool formation and allows for 'convection-moisture' feedbacks (Jeevanjee & Romps, 2013; Craig & Mack, 2013; C. J. Muller & Bony, 2015). Since the domain size is an important feature of the simulations we keep it fixed as we vary resolution, but this again limits the resolution range we can probe to $dx = 1, 2$, and 4 km. All simulations are initialized from an unaggregated state and run for 200 days.

Hovmoeller plots of precipitable water for these simulations (PW, units of mm, averaged over the 96 km dimension) are shown in Fig. S5. These plots show that the $dx = 1, 2$ simulations indeed aggregate, but that the 4 km simulation does not. This hints at a possible disinclination of simulations to aggregate at very *coarse* resolutions, a finding complementary to the resolution-dependence of aggregation at fine resolutions ($dx < 1$ km, C. J. Muller & Held, 2012; Yanase et al., 2020).

Figure S5 also shows cloud fraction profiles for these simulations (calculated as horizontal means, averaged over the last 40 days of simulation). The anvil cloud fractions are slightly smaller than for the corresponding fixed grid runs shown in Fig. 1b, which for $dx = 1, 2$ km is consistent with a slight reduction in cloud fraction due to aggregation (Wing, Emanuel, et al., 2017). Most notably for our purposes, however, the anvil fraction in the aggregated bowling-alley simulations *increases* from $dx = 2$ to $dx = 1$, similar to the unaggregated fixed grid runs in Fig. 1. Although such a small simulation set provides only a very preliminary test, these results do not point to a strong sensitivity of our results to aggregation or organization.

References

Bretherton, C. S., Blossey, P. N., & Khairoutdinov, M. F. (2005). An Energy-Balance Analysis of Deep Convective Self-Aggregation above Uniform SST. *Journal of the*

Atmospheric Sciences, *62*(12), 4273–4292.

Craig, G. C., & Mack, J. M. (2013). A coarsening model for self-organization of tropical convection. *Journal of Geophysical Research Atmospheres*, *118*(16), 8761–8769.

Cronin, T. W., & Wing, A. A. (2017). Clouds, Circulation, and Climate Sensitivity in a Radiative-Convective Equilibrium Channel Model. *Journal of Advances in Modeling Earth Systems*, 2883–2905.

Harrop, B. E., & Hartmann, D. L. (2016). The role of cloud radiative heating in determining the location of the ITCZ in aquaplanet simulations. *Journal of Climate*, *29*(8), 2741–2763.

Jeevanjee, N. (2017). Vertical velocity in the gray zone. *Journal of Advances in Modeling Earth Systems*, *9*, 2304–2316.

Jeevanjee, N., & Romps, D. M. (2013). Convective self-aggregation, cold pools, and domain size. *Geophysical Research Letters*, *40*(5), 994–998.

Jeevanjee, N., & Romps, D. M. (2018). Mean precipitation change from a deepening troposphere. *Proceedings of the National Academy of Sciences*, *115*(45), 11465–11470.

Krueger, S. K., Fu, Q., Liou, K. N., & Chin, H.-N. S. (1995, mar). Improvements of an Ice-Phase Microphysics Parameterization for Use in Numerical Simulations of Tropical Convection. *Journal of Applied Meteorology*, *34*, 281–287.

Lin, Y.-L., Farley, R. D., & Orville, H. D. (1983). *Bulk Parameterization of the Snow Field in a Cloud Model* (Vol. 22) (No. 6).

Lord, S. J., Willoughby, H. E., & Piotrowicz, J. M. (1984, oct). Role of a Parameterized Ice-Phase Microphysics in an Axisymmetric, Nonhydrostatic Tropical Cyclone Model.

Journal of the Atmospheric Sciences, *41*(19), 2836–2848.

Mlawer, E. J., Taubman, S. J., Brown, P. D., Iacono, M. J., & Clough, S. A. (1997, jul). Radiative transfer for inhomogeneous atmospheres: RRTM, a validated correlated-k model for the longwave. *Journal of Geophysical Research*, *102*(D14), 16663.

Muller, C. (2022). Spontaneous Aggregation of Convective Storms. *Annual Review of Fluid Mechanics*.

Muller, C. J., & Bony, S. (2015). What favors convective aggregation and why ? *Geophysical Research Letters*, 5626–5634.

Muller, C. J., & Held, I. M. (2012). Detailed Investigation of the Self-Aggregation of Convection in Cloud-Resolving Simulations. *Journal of the Atmospheric Sciences*, *69*(8), 2551–2565.

Muller, C. J., & Romps, D. M. (2018). Acceleration of tropical cyclogenesis by self-aggregation feedbacks. *Proceedings of the National Academy of Sciences*, *115*(12), 2930–2935.

Romps, D. M. (2008). The Dry-Entropy Budget of a Moist Atmosphere. *Journal of the Atmospheric Sciences*, *65*(12), 3779–3799.

Wing, A. A., Emanuel, K., Holloway, C. E., & Muller, C. (2017, feb). *Convective Self-Aggregation in Numerical Simulations: A Review.* Springer Netherlands.

Wing, A. A., & Emanuel, K. A. (2014). Physical mechanisms controlling self-aggregation of convection in idealized numerical modeling simulations. *Journal of Advances in Modeling Earth Systems*, *5*(November), 1–14.

Wing, A. A., Reed, K. A., Satoh, M., Stevens, B., Bony, S., & Ohno, T. (2017). Radiative-Convective Equilibrium Model Intercomparison Project. *Geoscientific Model Devel-*

opment Discussions, *11*(September), 1–34.

Wing, A. A., Stauffer, C. L., Becker, T., Reed, K. A., Ahn, M., Arnold, N. P., ... Zhao, M. (2020). Clouds and Convective Self-Aggregation in a Multi-Model Ensemble of Radiative-Convective Equilibrium Simulations. *Journal of Advances in Modeling Earth Systems*, 1–72.

Yanase, T., Nishizawa, S., Miura, H., Takemi, T., & Tomita, H. (2020). New Critical Length for the Onset of Self-Aggregation of Moist Convection. *Geophysical Research Letters*, *47*(16).

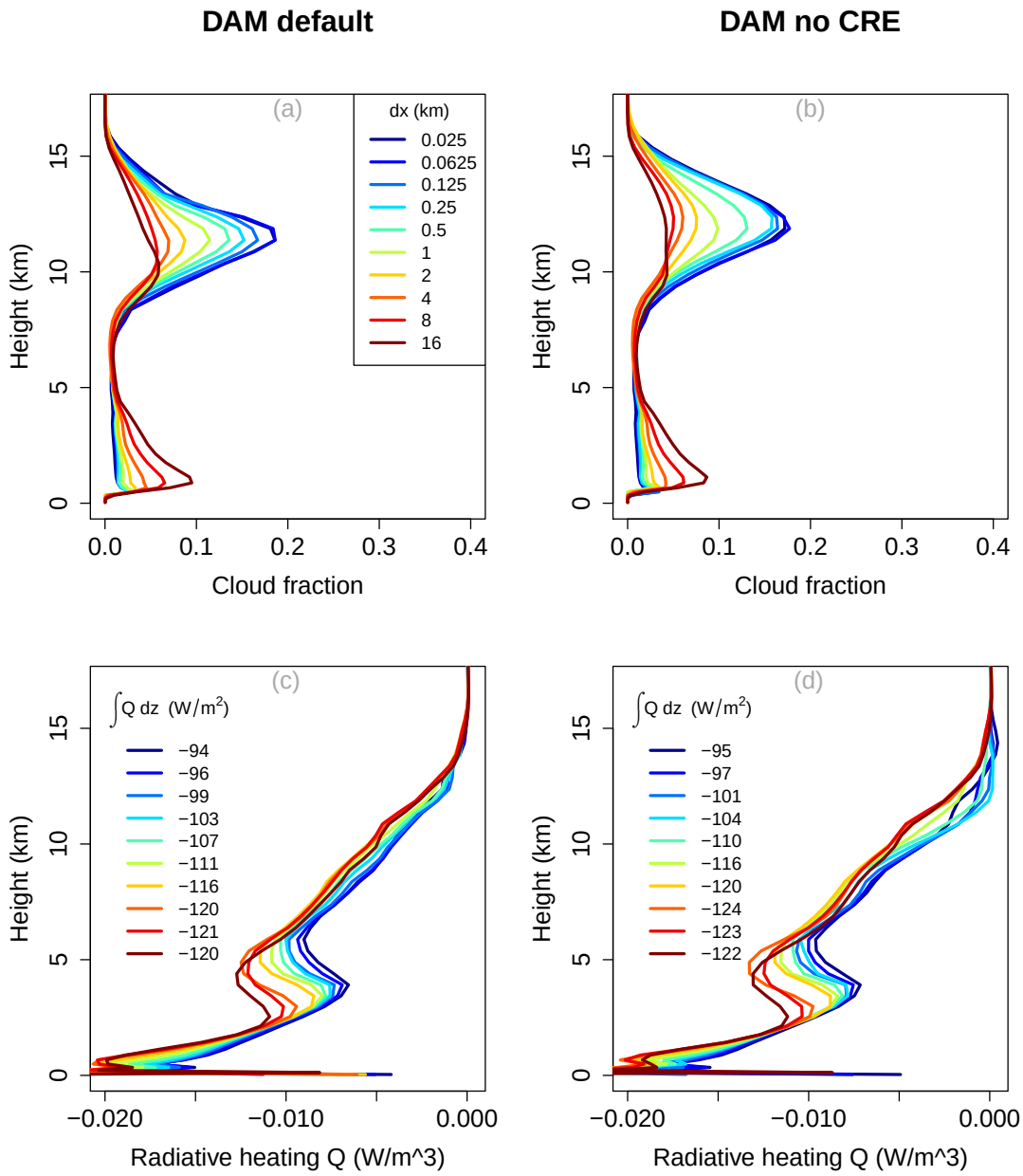

Figure S1. DAM also shows a marked dx-dependence of cloud fraction, which is not materially affected by cloud radiative effects (CRE). (a,c) Cloud fraction and radiative heating profiles (Q, W/m^3), from DAM RCE simulations at variable dx. Anvil cloud fractions vary by a factor of 4, whereas column integrated radiative heating ($\int Q\,dz$, W/m^2) varies by only 20% or so. **(b,d)** As in (a,c), but without CRE.

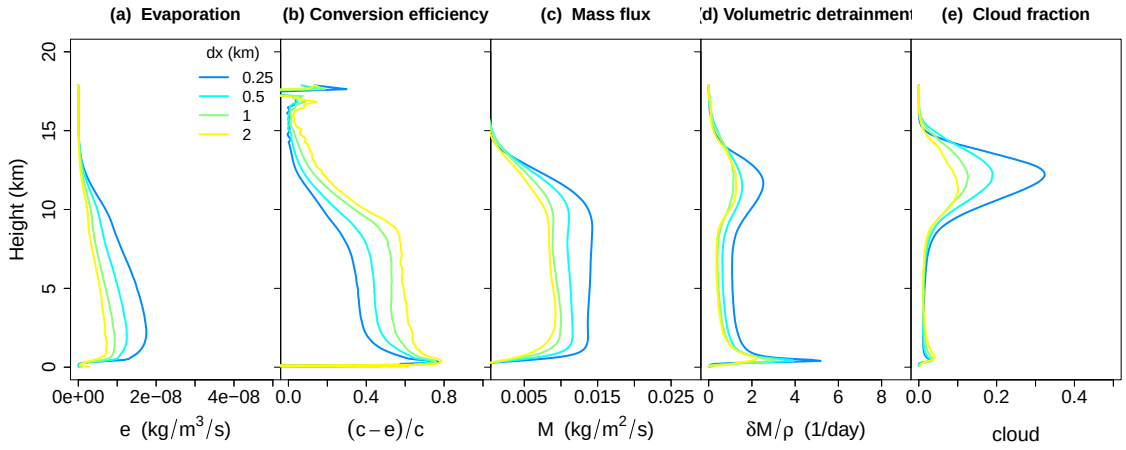

Figure S2. Fixed domain simulations behave very similarly to the fixed grid simulations. As in Fig. 2 of the main text, but for the fixed domain simulations. Despite a smaller number of simulations, a strong similarity to Fig. 2 of the main text is evident.

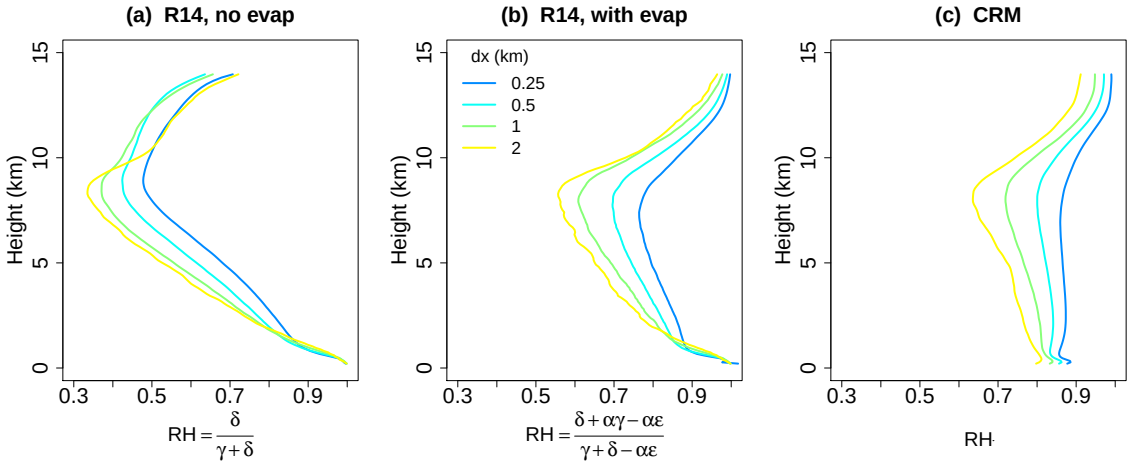

Figure S3. Fixed domain simulations behave very similarly to the fixed grid simulations. As in Fig. B.1 of the main text, but for the fixed domain simulations. Again, despite a smaller number of simulations, a strong similarity to Fig. B.1 of the main text is evident.

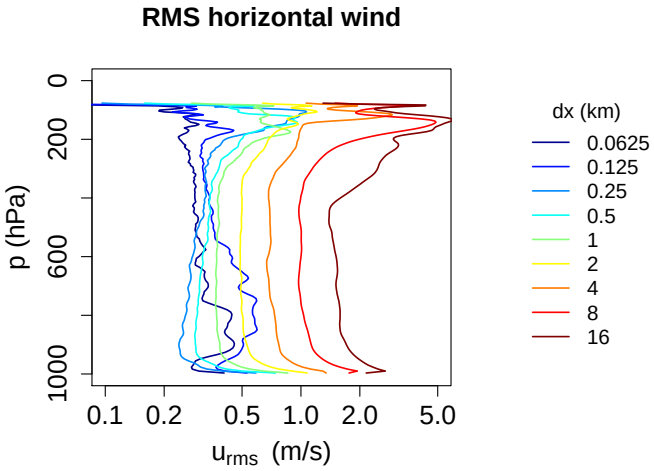

Figure S4. Simulated eddy wind speeds are largely $O(0.1$ m/s$)$. Profiles of u_{rms} for each simulation, calculated as standard deviations across horizontal dimensions and time from 14 days of daily snapshots.

dx (km)	w_0 (m/s)
0.0625	1
0.125	1
0.250	1
0.5	0.9
1	0.7
2	0.5
4	0.4
8	0.2
16	0.1

Table S1. Values of the vertical velocity threshold w_0 used to identify 'active' (i.e. updraft) cloudy regions.

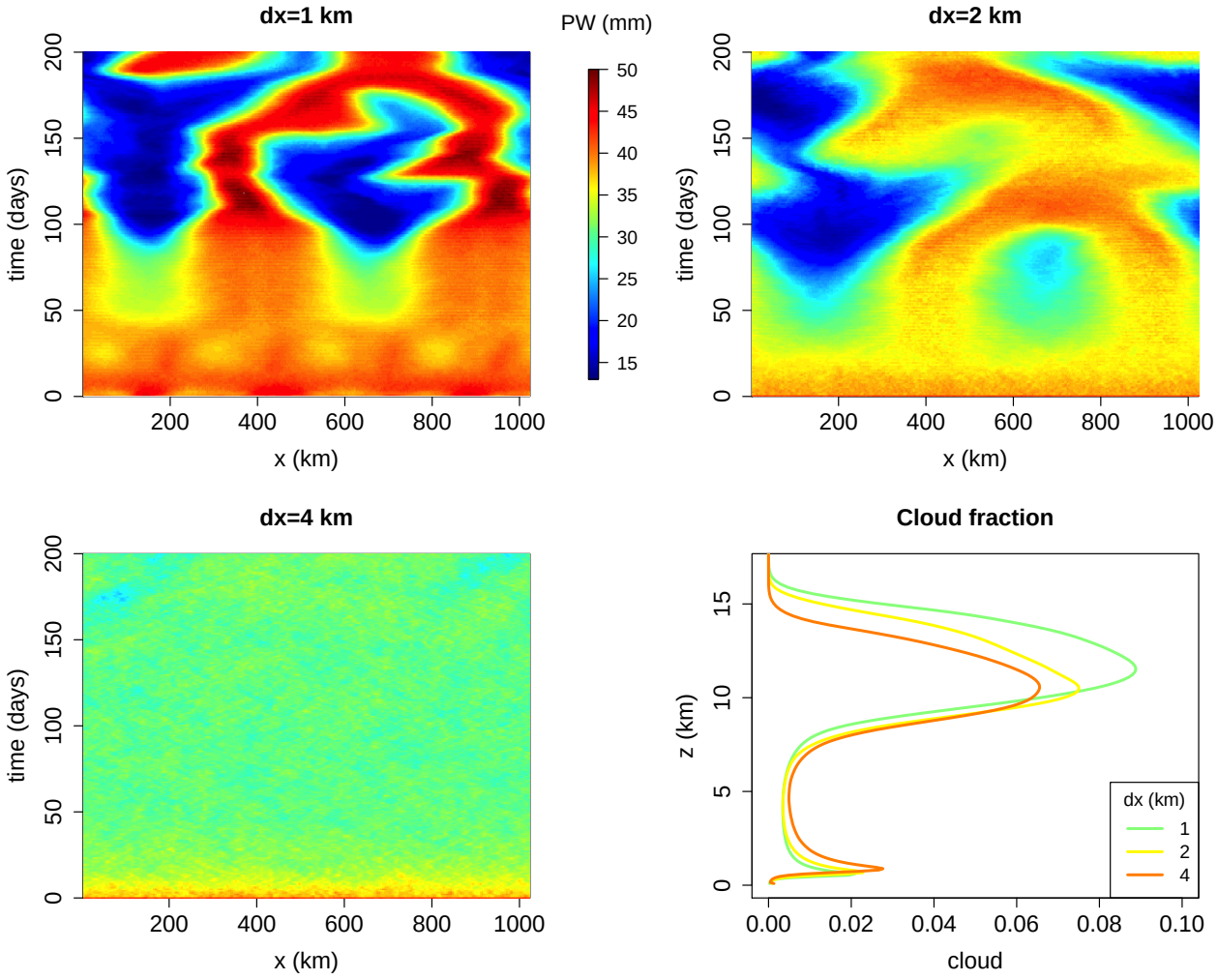

Figure S5. Aggregation occurs for $dx = 1, 2$ km but not $dx = 4$ km, with only minor effects on cloud fraction. Hovmoeller plots of precipitable water, as well as cloud fraction profiles, for our 'bowling-alley' simulations on a 1024×96 km^2 domain, with rain evaporation disabled to promote aggregation. The cloud fraction peaks are broadly similar to those in Fig. 1b, and show a similar increase with resolution.